

# Origin of the first order magnetostructural transition in $\text{YFe}_2\text{D}_{4.2}$

V. Paul-Boncour<sup>a,\*</sup>, M. Guillot<sup>b</sup>, G. André<sup>c</sup>, F. Bourée<sup>c</sup>,  
G. Wiesinger<sup>d</sup>, A. Percheron-Guégan<sup>a</sup>

<sup>a</sup> LCMTR, CNRS, 2-8 rue Henri Dunant, 94320 Thiais Cedex, France

<sup>b</sup> LCMI, CNRS-MPI, BP166, 38042 Grenoble Cedex 9, France

<sup>c</sup> LLB, CE-Saclay, 91191 Gif/Yvette, France

<sup>d</sup> IFP, T.U. Wien, Wiedner Hauptstrasse 8-10, 1040 Vienna, Austria

Received 6 September 2004; accepted 5 October 2004

Available online 7 July 2005

## Abstract

The deuterium order–disorder and the first order magnetic transitions in  $\text{YFe}_2\text{D}_{4.2}$  have been studied by X-ray and neutron diffraction, magnetization measurements and  $^{57}\text{Fe}$  Mössbauer spectroscopy. From 363 down to 290 K, a progressive lowering of the crystal symmetry from cubic to rhombohedral and then monoclinic structure is observed. At 290 K  $\text{YFe}_2\text{D}_{4.2}$  crystallizes in a primitive monoclinic space group  $P1c$  with  $a = 9.429(1) \text{ \AA}$ ,  $b = 11.474(1) \text{ \AA}$ ,  $c = 5.508(1) \text{ \AA}$ ,  $\beta = 122.37^\circ$ . This lowering of crystal symmetry leads to very different quantity of D neighbours around each Fe sites. The magnetic study shows that the moment of the Fe3 atoms, surrounded by nearly 5 D atoms, collapses at 84 K, leading to a transition from a ferromagnetic to an antiferromagnetic structure. The first order transition at 84 K is associated with a 0.55% volume decrease and the magnetization curves above 84 K display the same behaviour than the collective electron metamagnetism (CEM) observed in  $\text{RCO}_2$  compounds. This is related to the fact that for critical deuterium content between 4 and 5 D atoms in  $\text{YFe}_2$  the Fe 3d ferromagnetism becomes instable due to a strong modification of the electronic band structure.

© 2005 Elsevier B.V. All rights reserved.

**Keywords:** Hydrogen storage materials; X-ray diffraction; Neutron diffraction; Magnetic measurements; Mössbauer spectroscopy

## 1. Introduction

The study of the  $\text{YFe}_2\text{D}_x$  system has shown that deuterides with various deuterium content can be prepared from  $x = 1.3$  to 5 D/f.u. [1–4]. At room temperature these deuterides display a large variety of crystal structures related to a lowering of the cubic  $C15$  symmetry of  $\text{YFe}_2$  which are due to a preferential order of the deuterium atoms in the interstitial sites below a critical temperature  $T_S$  [5]. From  $x = 1.3$  to 3.5 the deuterides are characterized by a linear decrease of the Curie temperature  $T_C$  and a progressive increases of the Fe moment [1,5]. For  $x = 4.2$ , the compound is ferromagnetic up to 90 K, then display a sharp decrease of the magnetization through a first order transition [6]. For  $x = 5$  there is no more ordered Fe moment [4]. These results indicate that between  $x = 3.5$  and 5 the ferromagnetism of the Fe moment become unstable

due to the strong influence of the deuterium atoms on the electronic structure [7]. In addition, a previous work has showed that for  $x = 4.2$  the magnetic properties becomes very sensitive to the H/D isotopic effect, i.e. the first order magnetic transition is shifted from 90 to 140 K when the deuterium is substituted by hydrogen atoms [6]. In the present study we will report extended experimental results compared to those published in Ref. [6]. In order to understand the origin of this first order transition in  $\text{YFe}_2\text{D}_{4.2}$  the structural and magnetic properties of  $\text{YFe}_2\text{D}_{4.2}$  will be investigated by X-ray (XRD) and neutron powder diffraction (NPD), high magnetic field measurements and  $^{57}\text{Fe}$  Mössbauer spectroscopy.

## 2. Experimental

The preparation and characterization of single phase  $\text{YFe}_2$  and its deuterides is described in [6]. X-ray diffraction (XRD) measurements were done using a Bruker D8 diffractometer

\* Corresponding author. Tel.: +33 1 49781207; fax: +33 1 49781203.

E-mail address: paulbon@glvt-cnrs.fr (V. Paul-Boncour).

(Cu  $K\alpha$  radiation). An XRD pattern of  $YFe_2D_{4.2}$  at 290 K was also measured using synchrotron radiation ( $\lambda = 0.74744 \text{ \AA}$ ) provided on the Swiss-Norwegian beam line at the ESRF (Grenoble). The NPD experiments were performed at the LLB (Saclay), using the 3T2 and G4.1 diffractometers. The wavelengths were 1.2251 and 2.4266  $\text{\AA}$ , respectively. The magnetization measurements were performed using a high-magnetic field magnetometer ( $B \leq 23 \text{ T}$ ) at the LCMi (Grenoble). The  $^{57}\text{Fe}$  Mössbauer spectra were recorded between 4.2 and 300 K using a conventional constant acceleration type spectrometer. The data were analyzed by superposing a set of discrete Lorentzians with equal width. The quadrupole interaction was treated as a perturbation to the magnetic hyperfine interaction. The isomer shift data are given relative to the source (Fe(Rh)).

### 3. Results

The analysis of the XRD and NPD patterns indicates that two different transitions occur in different ranges of temperature: around room temperature (363 down to 280 K) there is an order–disorder transition due to the ordering of D atoms. No significant change is observed from 280 down to 160 K. Then from 150 down to 1.5 K the evolution of the patterns is related to different magnetic transitions. These two parts will be presented separately, starting from the highest symmetry towards the lower one: i.e. with decreasing temperature for the D disorder-order transition and with increasing temperature for the magnetic order.

#### 3.1. Deuterium order–disorder transition

The evolution of the NPD pattern of  $YFe_2D_{4.2}$  measured on the G4.1 spectrometer indicates a lowering of the crystal symmetry as the temperature ( $T$ ) decreases from 363 to 298 K. At 363 K the symmetry is cubic described by the  $Fd\bar{3}m$  space group ( $a = 7.95 \text{ \AA}$ ) with deuterium atoms in both  $A2B2$  ( $x_D = 3.8 \text{ D/f.u.}$ ) and  $AB3$  sites ( $x_D = 0.7 \text{ D/f.u.}$ ). Be-

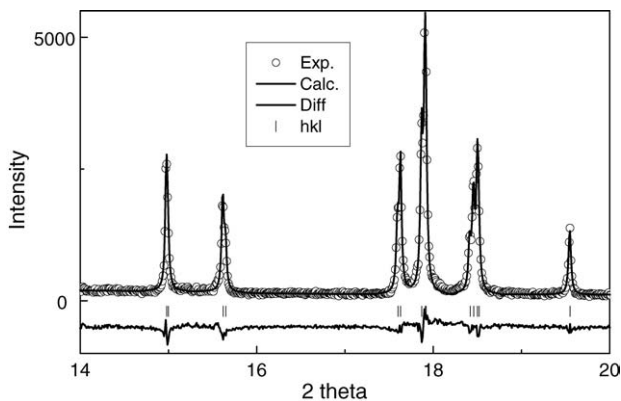


Fig. 1. XRD pattern of  $YFe_2D_{4.2}$  measured with synchrotron radiation and refined in the  $C2/m$  monoclinic space group.

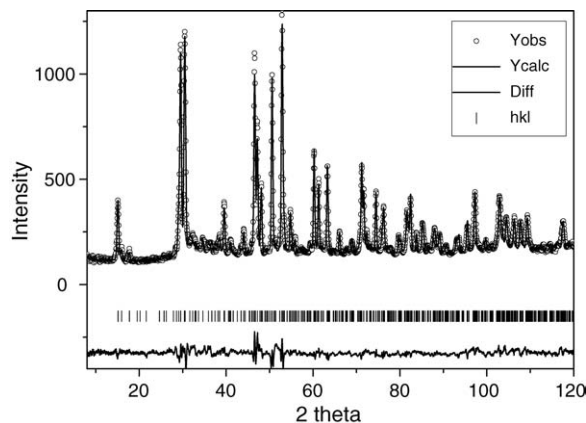


Fig. 2. Refinement of the NPD pattern of  $YFe_2D_{4.2}$  at 290 K measured on 3T2 spectrometer in the monoclinic structure ( $P21/a$ ) reported in Table 1.

low 340 K a rhombohedral distortion occurs and the pattern is refined in a rhombohedral space group with  $a = 5.702$  and  $c = 13.403 \text{ \AA}$ . As  $T$  decreases the rhombohedral distortion increases. At 295 K the XRD pattern measured by synchrotron radiation (Fig. 1) reveals an additional splitting of the lines due to the formation of a monoclinic structure described by the space group  $C2/m$  with  $a = 9.429(1) \text{ \AA}$ ,  $b = 5.737(1) \text{ \AA}$ ,  $c = 5.508(1) \text{ \AA}$ ,  $\beta = 122.37^\circ$  where  $b$  has the same value as the corresponding parameter  $a$  in the rhombohedral description ( $a = 5.737(1)$  and  $c = 13.220(1) \text{ \AA}$ ). In this centred monoclinic structure there is one Y site (4i) and three Fe sites (2d, 2b, 4f).

The corresponding NPD pattern measured on 3T2 at 300 K displays additional lines which can be refined using the primitive space group  $P21/a$  (Fig. 2 and Table 1). In this description

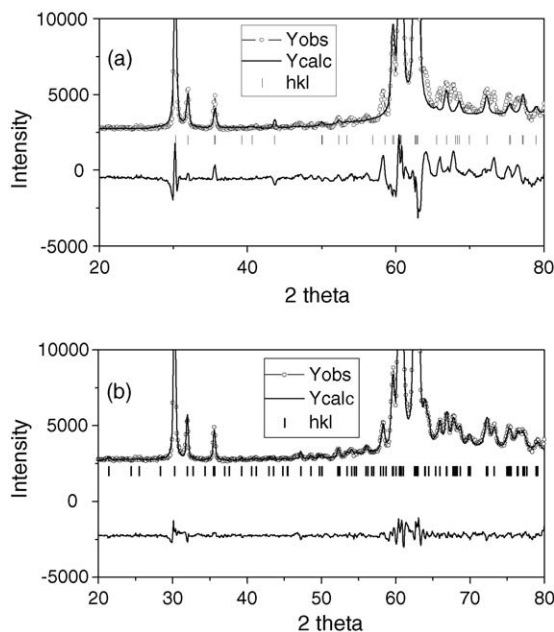


Fig. 3. NPD pattern of  $YFe_2D_{4.2}$  measured at 290 K on G4.1 spectrometer refined (a) with the structure described in Table 1 and (b) in a pattern matching mode with a doubling of the  $b$ .

Table 1  
Refined structure of YFe<sub>2</sub>D<sub>4.2</sub> measured at 300 K on 3T2

Atom (Wyckoff)	<i>x</i> ( $\delta x$ )	<i>y</i> ( $\delta y$ )	<i>z</i> ( $\delta z$ )	<i>B</i> ( $\delta B$ )	<i>N</i> ( $\delta N$ )
Y1 (4e)	0.8646	0.0	0.1226	1.04 (7)	1
Fe1 (2b)	0.5	0.0	0.5	1.13 (4)	1
Fe2 (2c)	0.5	0.0	0.0	1.13 (4)	1
Fe3 (4e)	0.25	0.25	0.5	1.13 (4)	1
D1 (4e)	0.858 (2)	−0.009	0.536 (5)		0.61 (3)
D2 (4e)	0.838 (3)	0.282 (4)	0.866 (6)		0.40 (3)
D3 (4e)	0.176 (1)	0.304 (2)	0.155 (3)		0.80 (3)
D4 (4e)	0.115 (2)	0.013 (1)	0.335 (6)		0.28 (2)
D5 (4e)	0.990 (123)	0.280 (185)	0.820 (225)	1.28 (7)	0.06 (6)
D6 (4e)	0.272 (6)	0.937 (6)	0.304 (6)		0.41 (3)
D7 (4e)	0.840 (3)	0.694 (4)	0.300 (4)		0.40 (3)
D8 (4e)	0.934 (5)	0.222 (8)	0.520 (9)		0.22 (9)
D9 (4e)	0.064 (5)	0.215 (5)	0.480 (6)		0.34 (9)
D10 (4e) (AB3)	0.712 (5)	0.000	0.635 (6)		0.33 (3)
D11 (4e) (AB3)	0.538 (0)	0.827 (0)	0.288 (0)		0.18 (9)
D (total)/f.u.					4.03 (1)
$R_F = 7.9\%$		$R_{B1} = 8.7\%$			

Monoclinic ( $P21/a$ ):  $a = 9.399(3) \text{ \AA}$ ,  $b = 5.740(3) \text{ \AA}$ ,  $c = 5.494(3) \text{ \AA}$ ,  $\beta = 122.22(3)^\circ$ ,  $V = 250.74(5) \text{ \AA}^3$ . The D1–D9 sites are A2B2 sites whereas the D10 and D11 are AB3 sites.

the Y and Fe sites occupy similar positions as in the space group  $C2/m$ , whereas 3.53 D atoms are located in nine over 12 possible A2B2 sites and 0.52 D in two over four AB3 sites. However a close examination of the 3T2 and G4.1 NPD patterns, shows the existence of additional lines which can be indexed by doubling the cell parameter  $b$  ( $b' = 2b$ ) (Fig. 3). This further lowering of the crystal symmetry can be described in the monoclinic space group  $P1c$ . But in this superstructure they are now 48 A2B2 sites and 16 non equivalent AB3 sites. With three positions and one occupancy factor per site this means 256 parameters to refine. Even taking into account the ordering already observed in the space group  $P21/a$  there are still 44 possible sites which becomes very difficult to refine with a powder pattern.

Nevertheless, an important result is that each Fe site (Table 2) is surrounded by a different quantity of deuterium atoms at distances between 1.5 and 2.8 Å: 3.2 D for Fe1, 4.4 D for Fe2 and 5.2 D for Fe3. This point, which has important consequences on the Fe magnetization will be discussed later.

The evolution of the cell parameters versus  $T$ , published previously in Fig. 2 of Ref. [6], shows that the parameter  $b'$  increases, whereas  $a$ ,  $c$  and  $\beta$  decrease on lowering the temperature. This evolution shows that the monoclinic distortion is related to an expansion along the  $b$  axis and that a particular D order should induces a doubling of the cell parameter along this direction.

### 3.2. Magnetic order

The NPD patterns measured at low temperature on G4.1 display two different behaviours: from 1.5 to 80 K the patterns do not reveal additional lines compared to the monoclinic structure and can be refined within a ferromagnetic structure. At 80 K the ferromagnetic line intensities sharply decreases as shown in Fig. 4 for the (001) line (at  $d = 4.63 \text{ \AA}$ ). From 80 to 132 K three additional magnetic lines are observed at  $d = 23.5$ , 5.51 and 3.98 Å, their intensity increasing up to 90 K and decreasing down to 130 K above this temperature

Table 2  
Coordination numbers and interatomic distances (Å) in YFe<sub>2</sub>D<sub>4.2</sub> at 300 K from the refinement in  $p21/a$  space group

Central atom	Y1	Fe1	Fe2	Fe3
Y1	2 at 3.402 1 at 3.468 1 at 3.519	2 at 3.300 4 at 3.365	2 at 3.122 4 at 3.351	2 at 3.154 2 at 3.317 2 at 3.382
Fe1	1 at 3.300 2 at 3.365		2 at 2.753	2 at 2.756
Fe2	1 at 3.122 2 at 3.351	2 at 2.753		2 at 2.866
Fe3	2 at 3.154 2 at 3.317 2 at 3.382	4 at 2.756	4 at 2.866	2 at 2.868
D (mean)	6.86 at 2–2.4	3.2 at 1.55–2.24	4.4 at 1.55–2.80	5.2 at 1.59–2.73

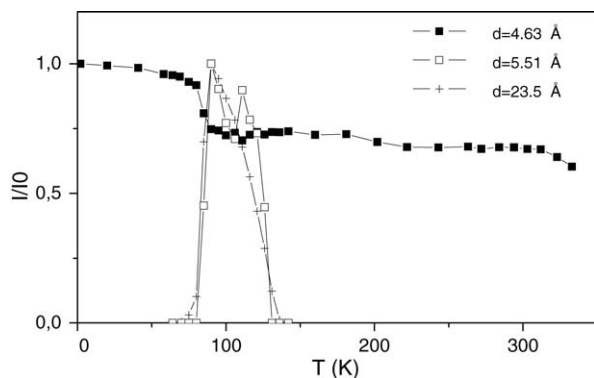


Fig. 4. Evolution of the line intensities corresponding to the ferromagnetic line at  $d = 4.63 \text{ \AA}$  and the two superstructure lines at  $d = 23.5$  and  $5.51 \text{ \AA}$ .

(Fig. 4). The superstructure lines can be indexed with a doubling of the  $b'$  parameter relative to the nuclear cell (e.g.  $4b$  compared to the cell refined by XRD). In this magnetic cell, the lines at  $23.5$  and  $5.51 \text{ \AA}$  are indexed as  $(0\ 1\ 0)$  and  $(3\ 1\ 0)$  line respectively. This corresponds to an antiferromagnetic structure with a propagation vector  $k = (0, 0.5, 0)$ . With only three magnetic lines it is difficult to completely solve this magnetic structure which contains 32 Fe atoms and we are looking for additional information delivered by Mössbauer spectroscopy.

The evolution of the Mössbauer spectra versus temperature reveals also three different behaviours (Fig. 5). From  $4.2$  to  $90 \text{ K}$  all the spectra could be sufficiently refined with eight sextets in agreement with the number of Fe sites in the monoclinic  $P1c$  superstructure with a wide distribution of hyperfine fields and isomer shifts. As  $T$  increases the mean hyperfine field decreases from  $23$  to  $19 \text{ T}$ . Between  $100$  and  $120 \text{ K}$ , the spectra have a more complex shape which can be explained by a superposition of doublets and sextets. At  $140 \text{ K}$ , e.g. the spectrum could be reasonably well fitted by superposing four sextets and four doublets (Fig. 5). The fact that the hyperfine field vanishes at different temperatures may indicate that the Fe atoms gradually lose their atomic moment, influenced by their specific local environment. From  $140$  to  $300 \text{ K}$  the spectra are dominated by a broadened nonsymmetric doublet. Taking into account the previous observation concerning the number of D neighbours around each Fe atom (Table 2) it is possible to assume that a larger amount of deuterium is responsible for a faster collapse of the hyperfine field and thus of the atomic moment. Since the Fe3 site is surrounded by 5 D atoms, it becomes very close to the magnetic instability and loses his moment before the Fe1 and Fe2 atoms. This is confirmed by experimental results and band structure calculations which have shown that in  $\text{YFe}_2\text{D}_5$  the Fe has no more ordered moment due to the strong Fe–H bonding and the filling of the conduction band [4,7]. The Fe3 site occupies the  $4e$  position in the middle of the cell. The Fe1 (2b) and Fe2 (2c) atoms are both surrounded by four Fe3 atoms and two Fe2 or two Fe1 atoms, respectively. If the Fe3 moment collapses, both Fe1 and Fe2 atoms lose four mag-

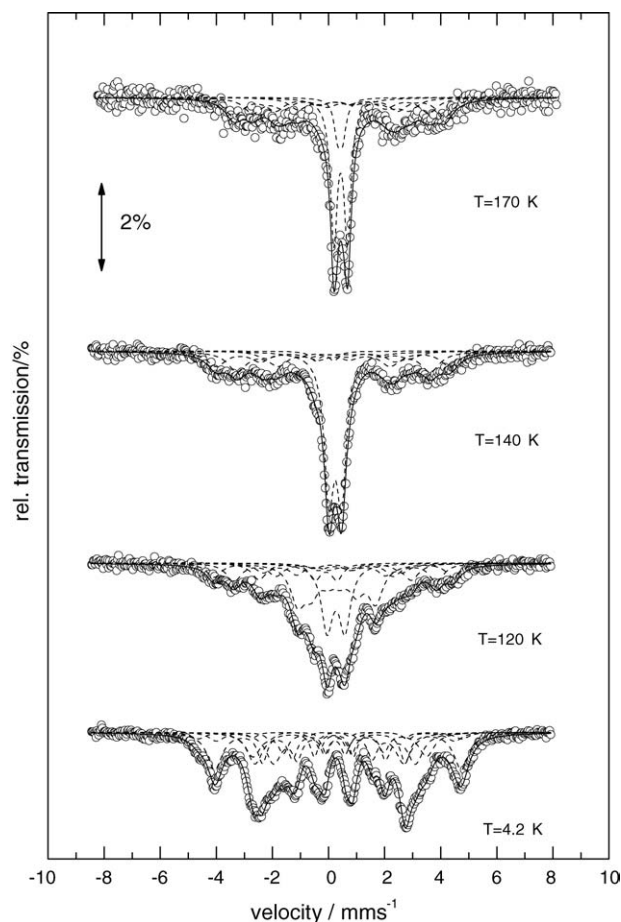


Fig. 5.  $^{57}\text{Fe}$  Mössbauer spectra recorded from  $\text{YFe}_2\text{D}_{4.2}$  at various temperatures. See comments in the text.

netic neighbours. Considering direct exchange interactions the Fe1 and Fe2 atoms have only two Fe neighbours bearing a Fe moment. They are forming linear chains separated of  $5 \text{ \AA}$  from each other. The magnetic part of the ND pattern above  $84 \text{ K}$  can be refined with a ferromagnetic coupling of the Fe1 and Fe2 atoms inside the nuclear structure with the Fe moment pointing in the  $\vec{a}$  direction. There is an inversion of the direction of the Fe moment in the second part of the magnetic cell ( $2b'$ ). Since the Fe1 and Fe2 atoms have only two magnetic neighbours instead of six compared to the ferromagnetic structure below  $80 \text{ K}$ , their moments decrease faster with raising the temperature than expected from a classical ferromagnet (Brillouin curve). Eventually, at  $140 \text{ K}$ , the magnetic interaction becomes too weak to keep a long range order and the compound is paramagnetic above the transition.

The evolution of the magnetization curves obtained in a high magnetic field above  $90 \text{ K}$  displays a metamagnetic behaviour (Fig. 4 of Ref. [6]). The extrapolation of the transition field  $H_m$  versus temperature for  $H = 0$ , leads to a critical temperature of  $84 \text{ K}$  (Fig. 6), in good agreement with the transition temperature observed in the NPD experiments (zero field measurements). The sharp decrease of  $0.55\%$  of the cell volume at  $84 \text{ K}$  [6] indicates that the first order magnetic

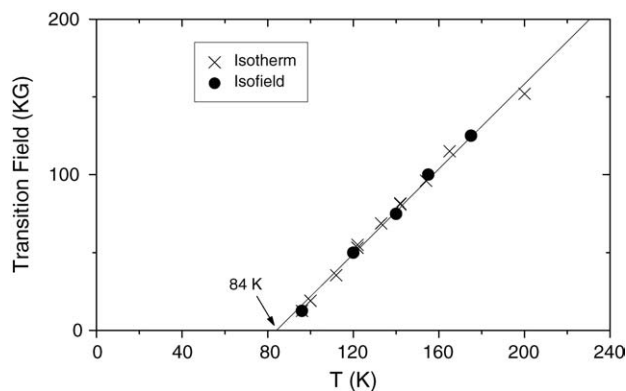


Fig. 6. Evolution of the transition field deduced from isofield and isotherm magnetization curves above 80 K.

transition is accompanied by a large magnetovolumic effect. This behaviour resembles the collective electron metamagnetism (CEM) observed in  $\text{RCO}_2$  compounds [8]. For  $\text{YCo}_2$  the metamagnetic transition is observed at 70 T at 4.2 K [9], but replacing Y by a heavy rare earth allows to decrease strongly the transition field and the critical temperature due to the strong internal molecular field. For example, in  $\text{HoCo}_2$ , the transition temperature at  $H = 0$  is near 80 K with a spontaneous magnetostriction of 0.55% [10]. This means that for the Fe3 atoms, the bonding with almost five hydrogen atoms modify its electronic structure which become close to the instability of ferromagnetism. In Ref. [7], band structure calculations have showed that for  $\text{YFe}_2\text{H}_5$  the Fe–H bonding becomes as important as the Fe–Fe bonding. The Fe 3d band is shifted towards the valence band leading to a decrease of the DOS at the Fermi level. The Stoner criterion is no more fulfilled and spin polarization does not occur.

#### 4. Conclusion

Deuterium order in  $\text{YFe}_2\text{D}_{4.2}$  leads to a lowering of the crystal symmetry from the cubic C15 structure above 363 K

down to a primitive monoclinic structure, with a doubling of the cell parameter along the  $b$  axis at 290 K. In the monoclinic structure the initial Fe site of the C15 structure is split in three different sites (Fe1, Fe2 and Fe3) with different quantity of D neighbours. From 1.5 to 75 K,  $\text{YFe}_2\text{D}_{4.2}$  is ferromagnetic. At 84 K it undergoes a first order magnetoelastic transition with a 0.55% decrease of volume. Above 84 K the magnetization is strongly field dependant and displays a collective electron metamagnetism like in  $\text{RCO}_2$  compounds. This transition can be attributed to the collapse of the Fe3 moments which are surrounded by about 5 D atoms, and are therefore very close from the ferromagnetic instability, like the Co moment in  $\text{RCO}_2$  compounds. Since the Fe1 and Fe2 atom have less D neighbours than Fe3, they still bears a moment and the magnetic structure becomes antiferromagnetic.

#### References

- [1] V. Paul-Boncour, L. Guénée, M. Latroche, M. Escorne, A. Percheron-Guégan, C. Reichl, G. Wiesinger, *J. Alloys Compd.* 253–254 (1997) 272.
- [2] V. Paul-Boncour, L. Guénée, M. Latroche, A. Percheron-Guégan, *J. Alloys Compd.* 255 (1997) 195.
- [3] V. Paul-Boncour, L. Guénée, M. Latroche, A. Percheron-Guégan, B. Ouladidaf, F. Bourée-Vigneron, *J. Solid State Chem.* 142 (1999) 120.
- [4] V. Paul-Boncour, S.M. Filipek, A. Percheron-Guégan, I. Marchuk, J. Pielaszek, *J. Alloys Compd.* 317–318 (2001) 83.
- [5] V. Paul-Boncour, A. Percheron-Guégan, *J. Alloys Compd.* 293–295 (1999) 237.
- [6] V. Paul-Boncour, G. André, F. Bourée, M. Guillot, G. Wiesinger, A. Percheron-Guégan, *Physica B* 350 (2004) e27.
- [7] V. Paul-Boncour, S. Matar, *Phys. Rev. B* 70 (2004) 184435.
- [8] D. Gignoux, D. Schmitt, in: Gschneidner Jr., K.A., Eyring, L. (Eds.), *Handbook of the Physics and Chemistry of Rare Earths*, vol. 20, Elsevier Science B.V., 1995, p. 293.
- [9] T. Goto, T. Sakakibara, K. Murata, H. Komatsu, K. Fukamichi, *J. Magn. Magn. Matter* 90–91 (1990) 700.
- [10] R. Minakata, M. Shiga, Y. Nakamura, *J. Phys. Soc. Jpn.* 41 (1976) 1435.